ACS OMEGA

http://pubs.acs.org/journal/acsodf

Article

In Situ Volume Recovery Method for Non-Seal Gas Pressure Measurement Technology: A Comparative Study

Chunlei Hua, Zhaofeng Wang,* Erlei Su,* Jiaxin Dong, Jiwei Yue, Yongjie Cui, and Kangjia Zhang

Cite This: *ACS Omega* 2022, 7, 41341−41352

Read Online

ACCESS | Metrics & More | Article Recommendations

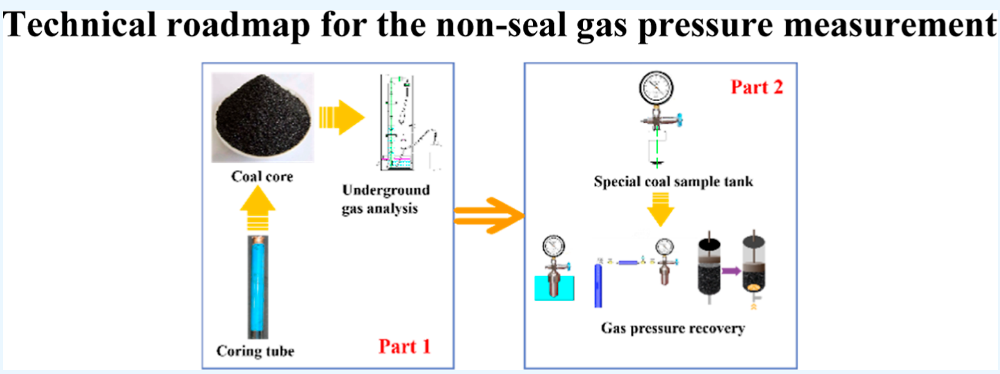

ABSTRACT: Coal seam gas pressure is one of the basic parameters for coalbed methane resource exploitation and coal mine gas disaster prevention. However, the present coal seam gas pressure measurement technology requires harsh field measurement conditions and a long testing period. In this study, a novel non-seal gas pressure measurement technology is proposed, and this technology is mainly aimed at three different changes before and after the collection of coal samples and realizes the real gas pressure measurement through the compensation of gas leakage, in situ volume recovery of the coal core, and reservoir temperature simulation. The technique not only can measure the original gas pressure of coal seam quickly and accurately but also does not need to seal the measuring hole. This paper focuses on the study of a key factor that affects the accuracy of non-seal gas pressure measurement: the restoration of in situ volume. Based on this, the influence of four different *in situ* volume recovery methods on the measurement accuracy is compared with the self-developed non-sealing gas pressure measuring system. Experimental results show that the *in situ* volume of the coal core cannot be completely restored by stress loading. Although the contact injection method can restore the original volume of the coal core, the pressure recovery error is large due to the replacement and displacement of the gas effect of water and the inclusion of the coal body effect of oil. Interestingly, the combination of stress loading and contact oil injection can not only restore the original volume of the coal core but also minimize the pressure recovery error, which is only less than 10%. Finally, based on the abovementioned experimental results, the *in situ* volume recovery method of non-seal gas pressure measurement technology is improved. Therefore, the research results of this paper provide a scientific basis for the field application of non-seal gas pressure measurement technology.

1. INTRODUCTION

China is the world's largest coal production and consumer.[1−4] At the same time, China is also the country with the most serious coal mine gas accidents in the world.[5−7] Among them, the proportion of outburst accident deaths in the total number of coal mine accidents gradually increases from 3.44% in 2001 to 6.58% in 2020.[8−10] It shows that gas accidents are still at a relatively high level and become more prominent in coal mine accidents.[11−14] The original gas pressure of the coal seam is one of the basic parameters for the study of the coal seam gas occurrence and emission law.[15−18] It is an important indicator of the danger degree of coal seam gas outburst and the difficulty degree of gas extraction, and it is the basis for coal seam gas prevention and control and coal seam gas extraction design.[19−21] Therefore, rapid and accurate measurement of gas pressure plays a vital role in coal mine safety production.

At present, gas pressure measurement methods can be roughly divided into the direct pressure measurement method and indirect pressure measurement method.[22−24] The direct pressure measurement method is to drill from the rock lane to

Received: August 10, 2022
Accepted: October 13, 2022
Published: November 1, 2022

the coal seam, to seal the hole with the sealing material, to draw the pressure measuring pipe from the drilling hole, and read out the coal seam gas pressure directly with the pressure gauge,[25,26] as shown in Figure 1. The key to affecting the reliability of the direct method pressure measurement results is the quality of the sealing holes. If the sealing methods such as clay sealing and cement mortar sealing are used, the filling cannot be fully filled, which will cause measurement errors. Form this, many scholars have conducted in-depth research on the direct pressure measurement method. Cui et al.[27] proposed a new gas pressure measurement method of water gas separation and preventing coal slime blockage, which solves the influence of water pressure, coal slime, and other factors on gas pressure estimation. Wang et al.[28] put forward a flexible gel sealing material and a novel active sealing method suitable for this material, and the experimental results show that this material and this method are superior to conventional sealing materials and traditional methods, respectively. Si et al.[29] proposed a gas pressure measurement method for water invasion drilling based on dissolved gas, and this provides a new idea for gas pressure measurement in water inrush coal seams.

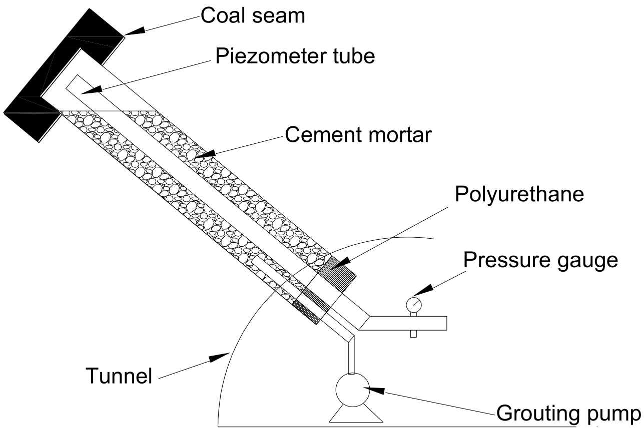

Figure 1. Direct measurement of coal seam gas pressure.

The indirect pressure measurement is a method to inverse the gas pressure from the gas content according to the Langmuir equation.[30] Skiba et al.[31] improved the accuracy of the indirect pressure measurement method by the use of an artificial neural network to estimate the value of selected sorption parameters of the coal-methane system. Wang et al.[32] combined the directional drilling system and special gas emission measuring device and applied the dynamic inversion model to measure coal seam gas pressure. Smith et al.[33,34] proposed the Smith−Williams desorption method to improve the accuracy of measuring gas pressure by the indirect method. In view of the problems existing in the prediction of coal seam gas pressure by the regression method, Wang et al.[35] put forward a new method of predicting deep coal seam gas pressure by the safety line method.

At present, both the direct method and the indirect method which are widely used have certain limitations. Under the gradual improvement of direct pressure measurement technology by many scholars, this method has been widely used. However, this method still has some limitations.[36] For example, the direct method of pressure measurement has strict requirements on the location of pressure measurement, and it is necessary to select the location where the rock gate or rock roadway is dense and not affected by geological structure, mining stress, gas drainage, and so forth. Moreover, this method is not suitable for the measurement of coal seam gas pressure after taking the measures of strengthening gas drainage.[37] Therefore, finding a method that can measure gas pressure accurately and quickly without any restriction of various conditions has become the goal of many gas disaster control workers.

In view of the technical problems encountered in the measurement of coal seam gas pressure, in this paper, a novel non-seal gas pressure measurement technology is proposed. Then, the feasibility of the technology and the main factors affecting the measurement accuracy are analyzed theoretically. Besides, the influence of four different *in situ* volume recovery methods on the measurement accuracy is compared with the self-developed non-sealing gas pressure measuring system, and the influence mechanism of the *in situ* volume recovery method on the measurement accuracy is discussed. Finally, based on the abovementioned experimental results, the *in situ* volume recovery method of non-seal gas pressure measurement technology is improved.

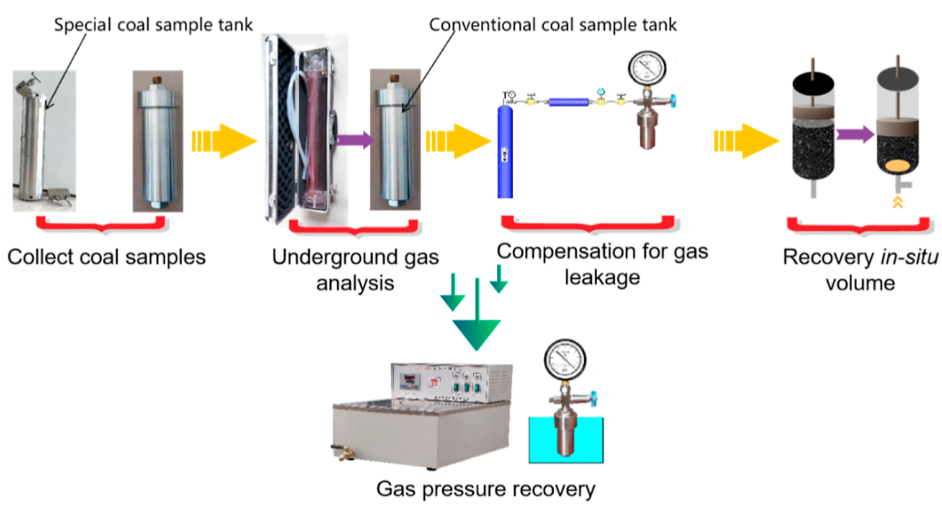

Figure 2. Technical route of the non-seal gas pressure measurement technology.

2. NON-SEAL GAS PRESSURE MEASUREMENT TECHNOLOGY

2.1. Principle of Non-Seal Gas Pressure Measurement Technology. The basic principle of the non-seal gas pressure measurement technology is based on three changes after the pressure measurement coal sample is collected from the underground coal seam occurrence conditions and loaded into the pressure measurement coal sample tank. First, during the process of the coal sample being exposed to loading into the coal sample tank, the gas desorption of the coal body leads to gas leakage. Second, the coal body changes from the dense block shape under the condition of the reservoir to the loose particle state, and the *in situ* volume changes occur. Third, the ambient temperature of the two states before and after the coal sample changes from the underground coal seam temperature to the test condition temperature is determined. According to the three different changes before and after the coal sample, the non-seal gas pressure measurement technology realizes the accurate and rapid determination of the gas pressure at the pressure measurement site through the compensation of gas leakage during coring, the recovery of coal core volume, and the simulation of reservoir temperature. Moreover, this technology has been proved to be feasible,[38] and the technical roadmap is shown in Figure 2.

2.2. Influencing Factors of Non-Seal Gas Pressure Measurement Technology. At present, the simulation of coal seam temperature can be realized using a constant temperature water bath, and the precise calculation of gas leakage can be realized by freezing coring,[39−42] but the recovery of coal core *in situ* volume has not yet been solved. Therefore, the *in situ* volume recovery of the coal core is the most crucial factor to ensure the accuracy of non-seal gas pressure measurement technology. The recovery of the *in situ* volume of the coal core is an important step to improve the accuracy of non-seal gas pressure measurement technology. Therefore, it is very important to analyze the causes of coal core *in situ* volume change and discuss the *in situ* volume restoration methods.

Under the original conditions, the coal is in a compact state, and when the original storage conditions change, its state will also change accordingly. As a result, the volume of the coal core taken out through drilling is not the volume in the original state. The causes of this phenomenon are as follows:

2.2.1. Sudden Release of Ground Stress. In the process of drilling and coring, the original storage conditions of coal seam are broken, resulting in the sudden release of *in situ* stress, which makes the coal in the reservoir transition from dense state to loose state, and the damage of coal body produces a large number of holes and cracks.

2.2.2. Human Factors during the Canning Process. When the extracted coal core is put into the coal sample tank, the coal structure is further destroyed, and the apparent volume of the coal core is increased, so that the coal core cannot be enriched in the coal sample tank and the free space is further expanded.

2.2.3. Mutual Support among Coal Particles. Coal is mainly composed of tightly packed crystallites, dispersed crystallites, and pores. After the coal sample is loaded into the coal sample tank, the coal samples are broken into different particle size states from the dense block type under reservoir conditions. The schematic diagram of the coal core volume state change before and after sampling is shown in Figure 3.

By analyzing the reasons for the change in the *in situ* volume of the coal core, it can be seen that compared with the coal under storage conditions, the coal core loaded into the coal sample tank generates more free space, which causes desorption of adsorbed gas, so as to reduce the gas pressure in the coal core. Therefore, in order to obtain accurate gas pressure, it is necessary to recover the *in situ* volume of the coal core. By calculating the volume change before and after sampling and then by filling the change volume of this part, the *in situ* volume recovery of the coal core can be realized.

Figure 3. Schematic diagram of coal core state changes before and after sampling.

2.3. *In Situ* Volume Recovery Method. According to the analysis of the reasons for the change in the *in situ* volume of the coal core, the following three kinds of methods to restore the *in situ* volume of the coal core are proposed.

2.3.1. Compressing Free Space. Due to the increase in excess space of the coal core after sampling, in order to realize the *in situ* coal core state, the volume of the coal sample in the coal sample tank can be compressed by stress loading, and the *in situ* volume recovery of the coal core can be realized by reducing the excess space of the coal cores. The schematic diagram is shown in Figure 4.

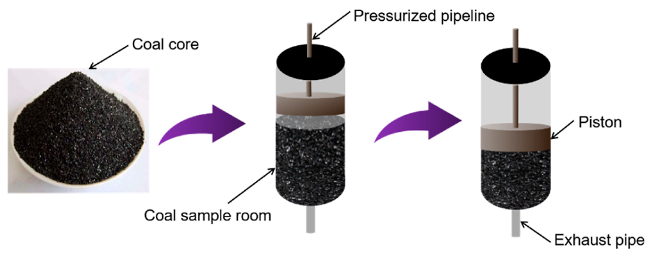

Figure 4. Schematic diagram of compressed free space.

2.3.2. Filling Free Space. The *in situ* volume recovery of the coal core can be realized by filling the free space in the coal core with gas, liquid, and solid injection into the coal sample tank. For the gas injection method, due to the large gas compressibility, it is difficult to ensure that the amount of injected gas is equal to the volume change in the coal core after gas injection. For the solid injection method, no matter how small the particle size of solid particles is, there will be gaps, and it is very difficult to inject solid particles into the coal core. For the liquid injection method, water and oil can be used for *in situ* volume recovery experiment of the coal core due to their small compressibility.[43,44]

2.3.3. Combination of Free Space Compression and Filling. The coal core can also be recovered *in situ* by stress loading and liquid injection. The recovery diagram is shown in Figure 5.

After research and discussion, the stress loading, contact liquid (water or oil) injection, and the combination of stress loading and contact liquid injection are finally selected to study the effect of *in situ* volume recovery of the coal core.

https://doi.org/10.1021/acsomega.2c05120
ACS Omega 2022, 7, 41341−41352

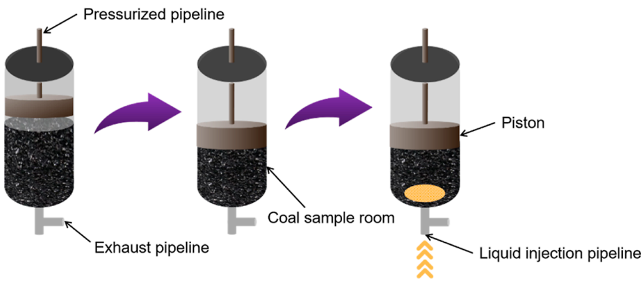

Figure 5. Legend of stress loading and contact liquid injection combination experiment.

3. EXPERIMENTAL SECTION

3.1. Determination Method of *In Situ* Volume. The coal samples used are anthracite coal collected from Guhanshan mine, Henan Province, China. Then, the coal samples were ground and sieved by metal sifters of different sizes to a particle size of less than 3 mm. Also, according to the determination of apparent relative density of coal (GB/6949-2010), the apparent relative density (ARD) of the coal sample is 1.51 g/cm^3.

The volume of the coal core under the condition of the coal seam reservoir can be described using formula 1

$$V_0 = \left(\frac{M}{\mathrm{ARD}} - \frac{M}{\mathrm{TRD}}\right) + \frac{M}{\mathrm{TRD}} = \frac{M}{\mathrm{ARD}} \tag{1}$$

where V_0 is the volume of the coal core under the condition coal seam reservoir, cm^3; M is the coal sample quality, g; ARD is the apparent relative density, g/cm^3; and TRD is the true relative density, g/cm^3.

The volume increase in the coal sample before and after sampling can be described using formula 2

$$\begin{aligned} \Delta V &= (V_2 - V_1) + (V_1 - V_0) \\ &= V_2 - V_0 \\ &= V_2 - \frac{M}{ARD} \end{aligned} \tag{2}$$

where ΔV is the *in situ* volume increase in the coal sample before and after sampling, cm^3; V_2 is the volume of the coal sample tank, 483.364 mL; and V_1 is the volume of the pressure measuring coal sample in the coal sample tank, cm^3.

3.2. Experimental Equipment. In order to realize the accurate and rapid determination of gas pressure at the pressure measurement site, the team independently developed the non-seal gas pressure measurement equipment. The schematic diagram of the experimental equipment is shown in Figure 6.

In order to determine the ideal coal core *in situ* volume recovery method, relying on the self-developed non-sealing coal seam gas pressure tester and pressure measuring tank (Figure 7), the experimental research on five different adsorption equilibrium pressures (0.31, 0.53, 0.74, 1.00, and 1.50 MPa) and four coal core *in situ* volume recovery methods (stress loading, contact water injection, contact oil injection, and the combination of stress loading and contact oil injection) is carried out.

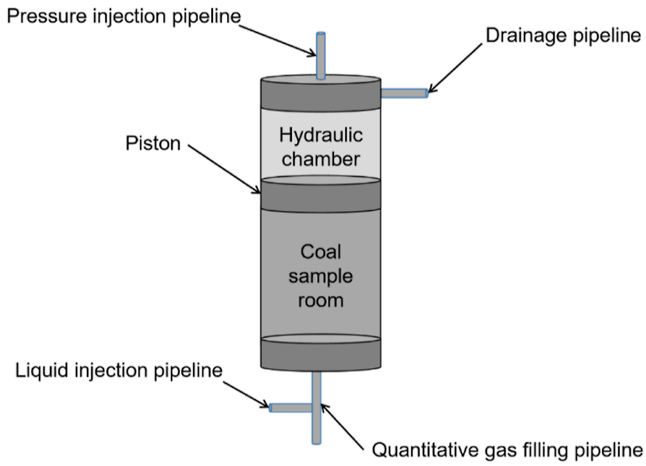

Figure 7. Schematic diagram of the coal sample tank.

3.3. Experiment Procedure. In order to achieve the best *in situ* volume restoration effect, four restoration methods such as stress loading, contact water injection, contact oil injection, and combination of stress loading and contact oil injection are proposed according to the experimental principle for related experiments and discussions.

3.3.1. Stress Loading. After sampling, the porosity of the coal core increases, that is, the free space increases. The *in situ* porosity can be recovered by eliminating the excess free space. First, the constant temperature water bath is set as 30 °C for cyclic operation, providing a constant temperature environment for the coal sample. Then, the constant pressure working mode is set as 20.00 MPa, the liquid is sucked and discharged circularly through the constant speed and constant pressure pump to continuously inject water and pressurize the hydraulic chamber

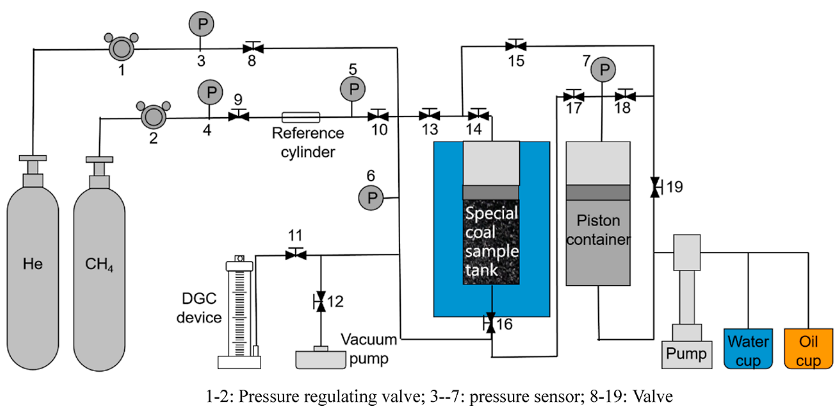

Figure 6. Schematic drawing of non-seal gas pressure measurement equipment. 1−2: pressure regulating valve; 3−7: pressure sensor; and 8−19: valve.

https://doi.org/10.1021/acsomega.2c05120
ACS Omega 2022, 7, 41341−41352

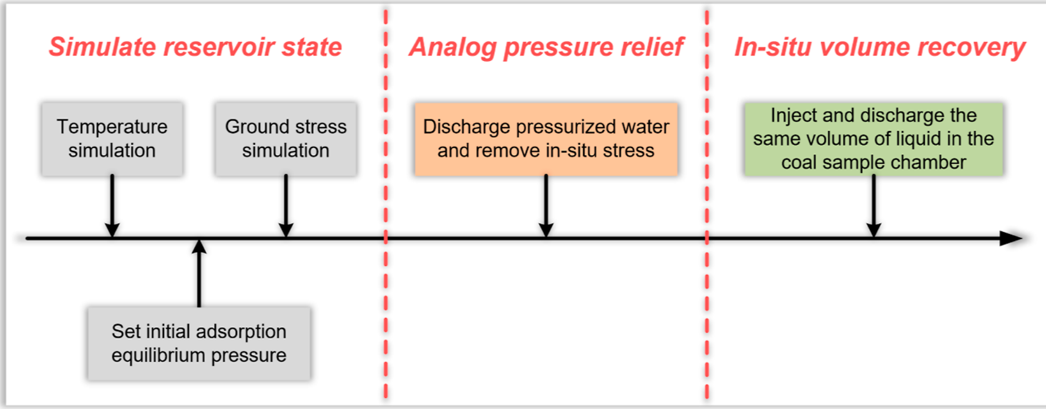

Figure 8. Experimental procedure of *in situ* volume recovery by contact injection.

in the upper chamber of the piston coal sample tank, and the piston is pushed down to compress the coal sample. Then, the cumulative flow is the compensation amount of the *in situ* volume increase in the coal core under this pressure.

According to formula 2, after taking out 380 g of the coal core, the *in situ* volume increase is 231.708 mL. In order to explore how much stress should be applied to fully compensate the *in situ* volume increase in the coal core, experiments are carried out under different pressures (5.00, 10.00, 15.00, ... 65.00 MPa) to compensate the *in situ* volume increase in the coal core.

3.3.2. Contact Water/Oil Injection. The excess free space of the coal core is filled by contact water/oil injection to realize the *in situ* volume recovery of the coal core. Taking the buried depth of 800 m coal sample as an example, under the 20.00 MPa overburden pressure and 30 °C constant temperature water bath environment, the gas is filled into the coal sample tank with 380 g of the coal sample, and the initial adsorption equilibrium pressures are set as 0.31, 0.53, 0.74, 1.00, and 1.50 MPa. The state of the coal sample at this time is taken as its state under reservoir conditions. The liquid discharged by unloading overburden pressure is collected, and the volume of the liquid(ΔV) is the increase in the *in situ* volume of the coal sample "before and after sampling". Then, quantitative (ΔV) water/oil is injected into the hydraulic chamber of the lower chamber of the coal sample tank to achieve re-adsorption equilibrium. The gas pressure recovery results (P_s) are observed and compared with the initial adsorption equilibrium pressure (P_0) to determine whether the *in situ* volume recovery method of the coal core with contact water/oil injection is feasible. The general experimental procedure is shown in Figure 8.

3.3.3. Combination of Stress Loading and Contact Oil Injection. When using this method to restore the coal core *in situ* volume, the sequence of oil injection before pressurization is selected. The lower chamber is filled with oil to compensate for the part of the *in situ* volume increase, and then, the upper chamber is pressurized to compensate for the remaining *in situ* volume increase. Through these two steps, the original volume of the coal core is completely restored.

4. RESULTS AND DISCUSSION

4.1. Stress Loading Only. To eliminate the test error and the contingency of the experiment, four groups (group I, group II, group III, and group IV) of the same experiments are carried out in this part of the study. The experimental data satisfy the formula $Q = A \times B \times \delta/(1 + B \times \delta)$, where A is the limit *in situ* volume compensation when B approaches infinity. The parameters in the formula are shown in Table 1. The relationship curve between the stress loading value and the *in situ* volume compensation of the coal core is fitted, and then, the pressure loading value required when the *in situ* volume increase in the coal core is 231.708 mL is obtained by inversion. The relationship curve between the *in situ* volume compensation and the loading burden is shown in Figure 9.

Table 1. Function Fitting Parameter Results

	I	II	III	IV
A	234.16749	233.92081	233.82847	233.85791
B	0.40969	0.41222	0.40471	0.41875
δ/MPa	229.954	254.020	270.000	257.375
$\overline{\delta}$/MPa	252.837			

According to the fitting formula, when the *in situ* volume increase in the coal sample is completely restored, the stress to be applied is about 252.837 MPa.

In fact, it is unrealistic to use the stress loading value calculated by the fitting function to compensate the *in situ* volume increase, but through research and analysis, it is found that this method can achieve 90% of the *in situ* volume recovery effect of the coal core. The reasons are as follows.

(1) When the applied overburden pressure is about 252.837 MPa, an equivalent force of 2.53×10^5 KN per square meter is required, which extremely demands for the compressive strength and instrument accuracy of the whole experimental equipment and equipment and is very difficult to manufacture.

(2) The predicted pressure values are not universal when the free space increase in coal samples is fully compensated, which may be limited to the types of coal used in the experiment, which may be due to the difference of the predicted *in situ* volume recovery pressure values of coal cores of different types and qualities.

(3) From the theoretical point of view, after the coal sample is loaded into the coal sample tank, the coal samples are broken into different particle size states from the dense block type under reservoir conditions. Under pressure, due to the mutual support between different particles to resist the recovery of coal core volume, the new pores and cracks due to coal crushing cannot be completely "healed".[45−48]

https://doi.org/10.1021/acsomega.2c05120
ACS Omega 2022, 7, 41341−41352

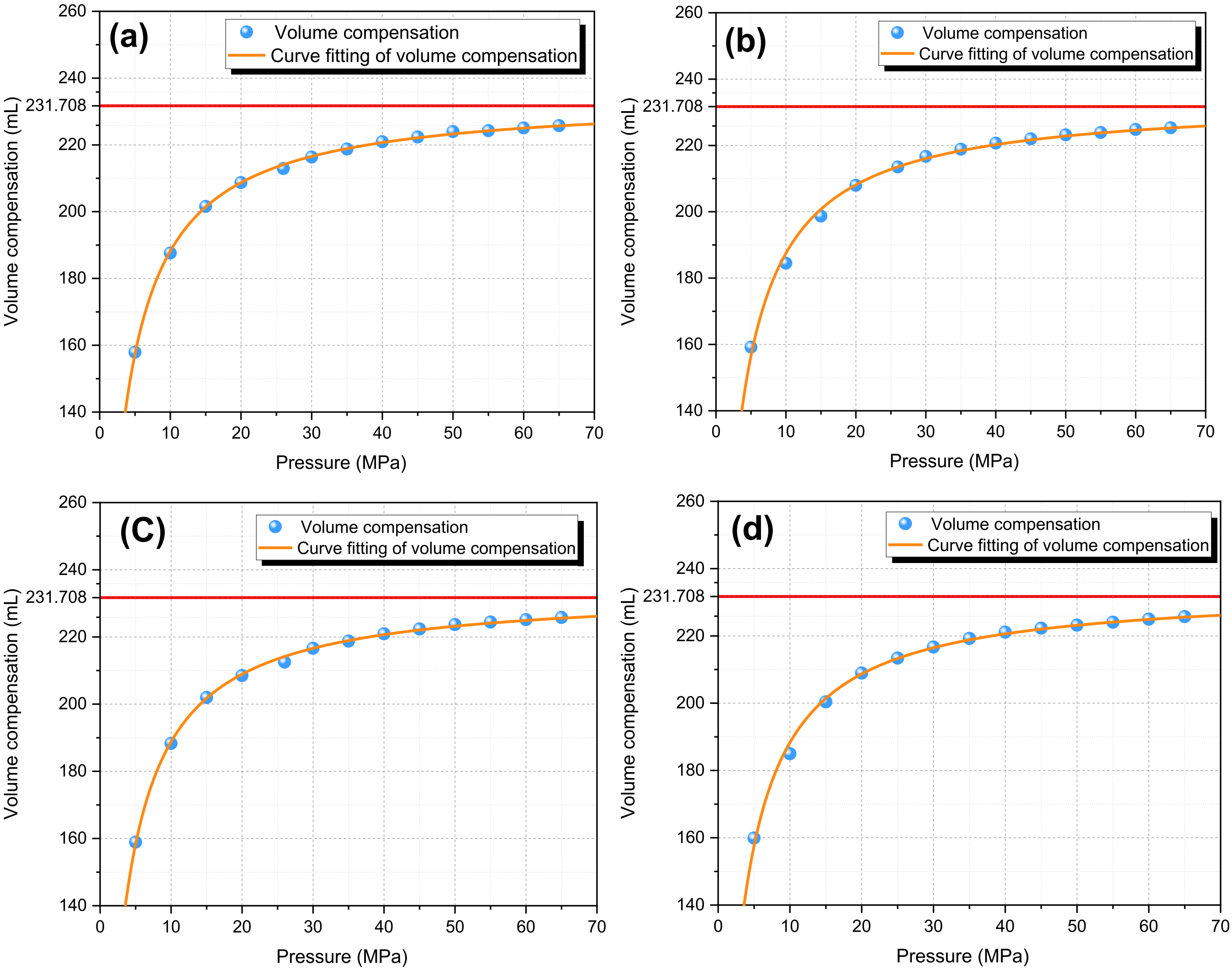

Figure 9. Relationship between *in situ* volume increase compensation and overburden pressure: (a) group I, (b) group II, (c) group III, and (d) group IV.

Therefore, no matter from the technical or theoretical analysis, it is not advisable to restore the coal core *in situ* volume only by means of stress loading.

4.2. Contact Water Injection. Table 2 shows the pressure relief liquid collection volumes of the five adsorption equilibrium pressures, and the gas pressure recovery curve after the *in situ* volume recovery of the coal after contact water injection is shown in Figure 10.

Table 2. Pressure Relief Collection Volume of Adsorption Equilibrium Pressures

pressure (MPa)	0.31	0.53	0.74	1.00	1.50
ΔV (mL)	175.0	173.6	174.5	171.6	174.3

The recovery result (P_S) of each pressure and its error with the corresponding initial adsorption equilibrium pressure (P_0) are shown in Table 3 and Figure 11.

From the abovementioned experimental research results, it can be seen that the overall error range between the gas pressure recovery value (P_S) after the *in situ* volume recovery of the coal core by contact water injection and the corresponding initial adsorption equilibrium pressure (P_0) is between 40.67 and 116.13%, and the pressure recovery effect after the *in situ* volume recovery of coal core by contact water injection decreases with the increase in adsorption equilibrium pressure.

For the following reasons, it is not advisable to conduct *in situ* volume recovery of the coal core only through contact water injection.

(1) When water is injected into the coal sample tank during the adsorption equilibrium state, the original gas adsorption equilibrium state in the system will be broken, and the water will replace the adsorbed gas and convert the adsorbed gas into free gas. The final pressure recovery value will increase due to the increase in the amount of free gas.[49,50] The schematic diagram of water molecules replacing adsorbed methane molecule is shown in Figure 12.

(2) When the *in situ* volume of the coal core is restored by injecting liquid into the coal sample chamber, the injected liquid will drive the free gas to the top of the coal sample chamber and form a certain thickness of the liquid level at the top of the coal sample, making it difficult for the free gas at the top to enter the coal sample. The schematic diagram of this restoration method is shown in Figure 13. As a result, the displaced free gas cannot be re-adsorbed and transformed into the adsorbed state,[51] resulting in the

https://doi.org/10.1021/acsomega.2c05120
ACS Omega 2022, 7, 41341−41352

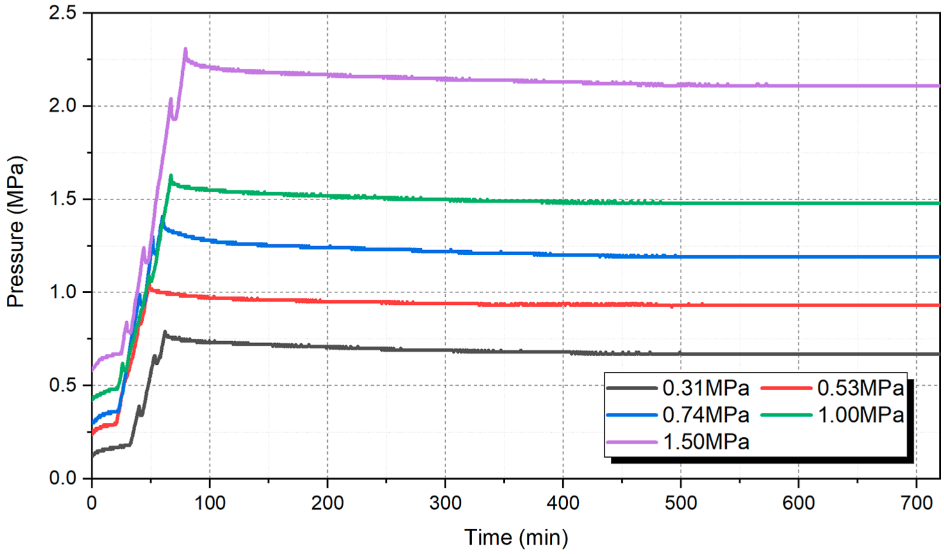

Figure 10. Comparison of pressure recovery curves under the contact water injection mode.

Table 3. Results of Contact Water Injection Gas Pressure Recovery

initial pressure (MPa)	0.31	0.53	0.74	1.00	1.50
recovery pressure (MPa)	0.67	0.93	1.19	1.48	2.11
pressure error (%)	116.13	75.47	60.81	48.00	40.67

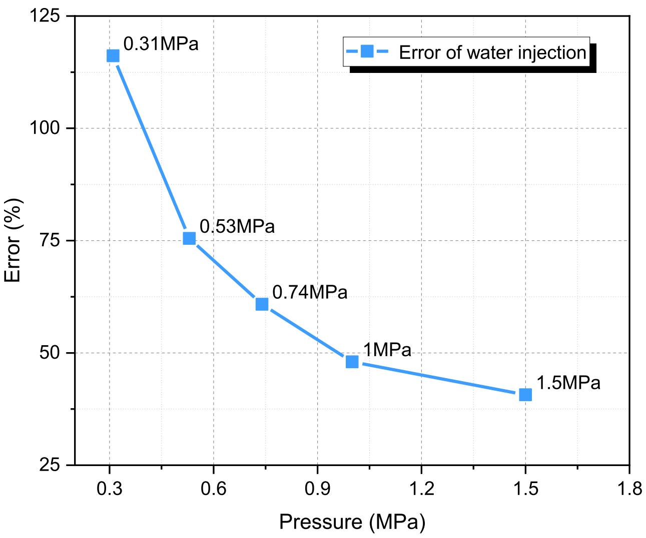

Figure 11. Relationship between the pressure error and initial adsorption equilibrium pressure.

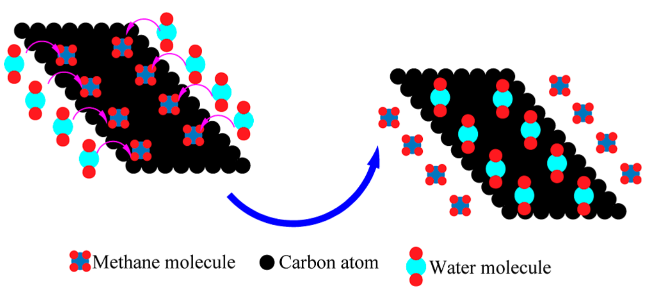

Figure 12. Diagram of displacement adsorption.

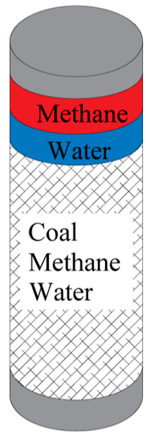

Figure 13. Schematic diagram of *in situ* volume recovery of the contact water coal core.

gas pressure recovery value being larger than the initial adsorption equilibrium pressure.

The experimental results show that the experimental error of restoring the *in situ* volume of the coal core by the contact water injection decreases with the increase in adsorption equilibrium pressure. The reason is that the density of adsorbed methane increases with the increase in pressure, when the injected water interacts with the adsorbed methane in pores of different sizes, and replacing the same volume of adsorbed methane under high pressure will produce more free methane than under low pressure.[52−55] The greater the gas pressure is, the more the free gas is.[56] The proportion of the amount of free gas increased by water displacement to the amount of free gas at the initial adsorption equilibrium also decreases with the increase in adsorption equilibrium pressure, and the recovery value of gas pressure is relatively closer to the initial adsorption equilibrium pressure. Therefore, the experimental error decreases with the increase in adsorption equilibrium pressure.

4.3. Contact Oil Injection. The gas pressure volume curve after *in situ* recovery of the contact oil injection core is shown in Figure 14.

https://doi.org/10.1021/acsomega.2c05120
ACS Omega 2022, 7, 41341−41352

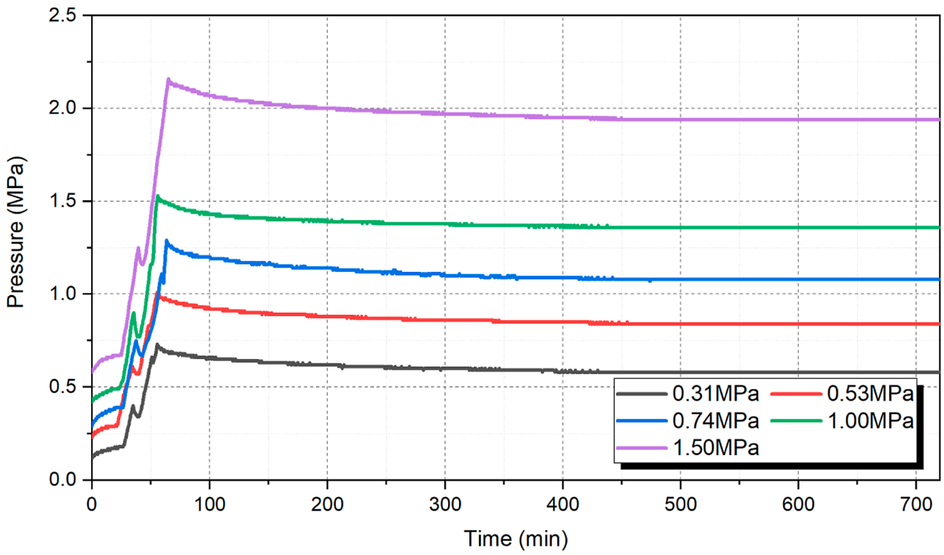

Figure 14. Comparison of pressure recovery curves under the contact oil injection mode.

The recovery result (P_S) of each pressure and its error with the corresponding initial adsorption equilibrium pressure (P_0) are shown in Table 4 and Figure 15.

Table 4. Results of Contact Oil Injection Gas Pressure Recovery

initial pressure (MPa)	0.31	0.53	0.74	1.00	1.50
recovery pressure (MPa)	0.58	0.84	1.08	1.36	1.94
pressure error (%)	87.10	58.49	45.95	36.00	29.33

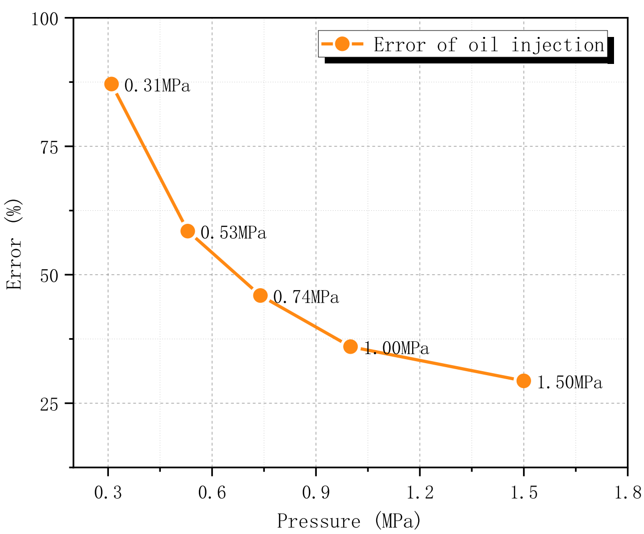

Figure 15. Relationship between the pressure error and initial adsorption equilibrium pressure.

According to the abovementioned research results, the overall error range between the gas pressure recovery value (P_s) after the *in situ* volume recovery of the contact oil injection core and the corresponding initial adsorption equilibrium pressure (P_0) is between 29.33 and 87.10%, which is larger than the corresponding initial adsorption equilibrium pressure, and the experimental pressure recovery error of the volume of oil injection decreases with the increase in adsorption equilibrium pressure.

It can be found from the experimental results that the gas pressure recovery value of the *in situ* volume of the coal core recovered by the contact oil injection is generally larger. This is because in the process of oil injection at the lower end of the coal sample chamber to recover the *in situ* volume of the coal core, the free gas will be driven to the top of the coal sample chamber. When the oil injection is completed, a certain thickness of the liquid surface is formed at the uppermost end of the coal sample to isolate the path of free gas from the top into the coal sample, and the injected silicone oil is attached to the surface of the coal sample particles, which has a strong wrapping effect on the coal sample particles, closing the adsorption path of the coal sample to the gas and making it more difficult to adsorb the gas (as shown in Figure 16), resulting in an increase in the content of free gas compared with the initial state during the re-adsorption equilibrium, which shows that the recovery value of gas pressure is larger than the initial adsorption equilibrium pressure.

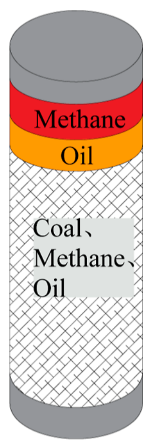

Figure 16. Schematic diagram of *in situ* volume recovery of the contact oil coal core.

4.4. Combination of Stress Loading and Contact Oil Injection. After the *in situ* volume recovery of the coal core by the combination of contact oil injection and stress loading, the coal sample can be adsorbed and balanced again in the constant

https://doi.org/10.1021/acsomega.2c05120
ACS Omega 2022, 7, 41341−41352

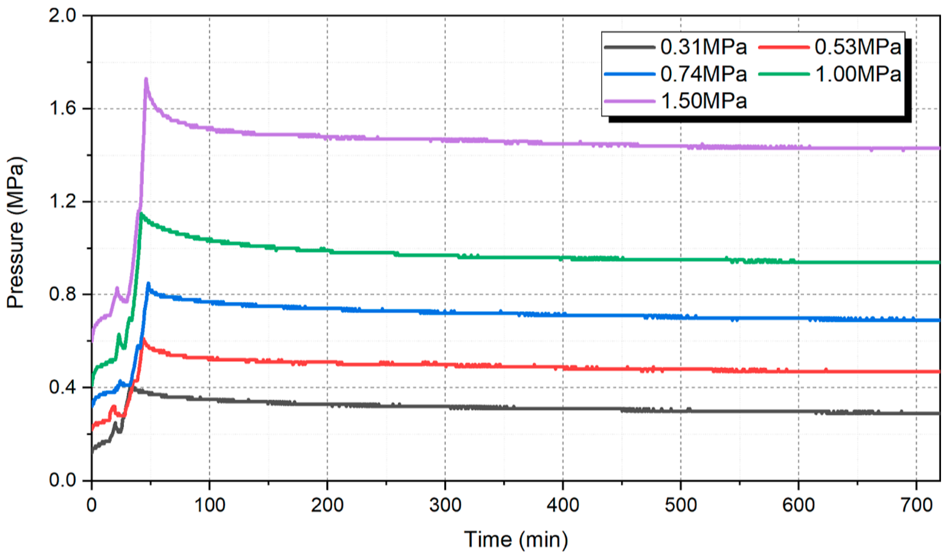

Figure 17. Comparison of pressure recovery curves under contact oil injection/stress loading.

temperature water bath environment. The gas pressure recovery curve is shown in Figure 17.

The recovery result (P_S) of each pressure and its error with the corresponding initial adsorption equilibrium pressure (P_0) are shown in Table 5 and Figure 18.

Table 5. Results of Contact Oil Injection/Stress Loading Gas Pressure Recovery

initial pressure (MPa)	0.31	0.53	0.74	1.00	1.50
recovery pressure (MPa)	0.34	0.57	0.78	1.04	1.54
pressure error (%)	9.68	7.55	5.41	4.00	2.67

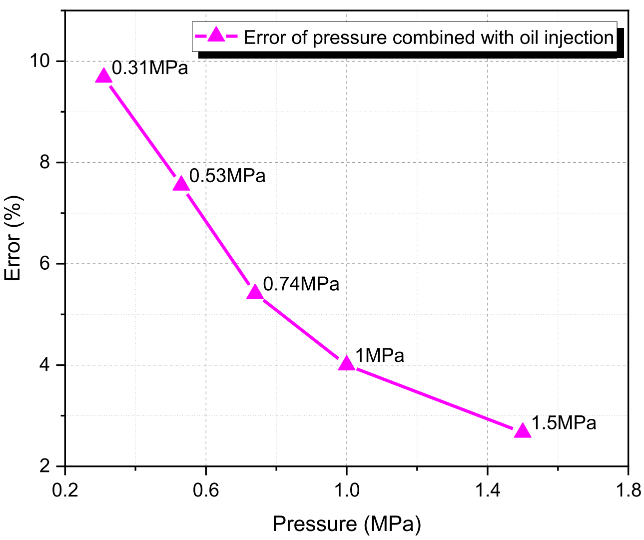

Figure 18. Relationship between the pressure error and initial adsorption equilibrium pressure.

It can be seen from the abovementioned research results that the overall error range between the gas pressure recovery value (P_S) and the corresponding initial adsorption equilibrium pressure (P_0) after restoring the *in situ* volume of the coal core by the combination of contact oil injection and stress loading is between 2.67 and 9.68%.

It can be seen from Figure 18 that the test results of the combination of stress loading and contact oil injection are also slightly larger, because a small amount of injected silicone oil comes into contact with a small part of the coal sample and adheres to its surface, which makes this part of the wrapped coal sample particles unable to participate in the adsorption of free gas.[57] The decrease in the number of truly effective coal samples leads to the decrease in the free gas amount adsorbed relative to the initial adsorption equilibrium state, and the free gas amount increases relative to the equilibrium state again, so the pressure recovery value is slightly larger.

4.5. Comparison and Selection of *In Situ* Volume Recovery Methods. The *in situ* volume recovery of the coal core is carried out by three methods, the contact water injection, the contact oil injection, the combination of contact oil injection and stress loading. Moreover, the error relationship between the initial adsorption equilibrium pressure and the pressure recovery result is shown in Figure 19.

According to the abovementioned test results, it is found that the *in situ* volume of the coal core cannot be completely

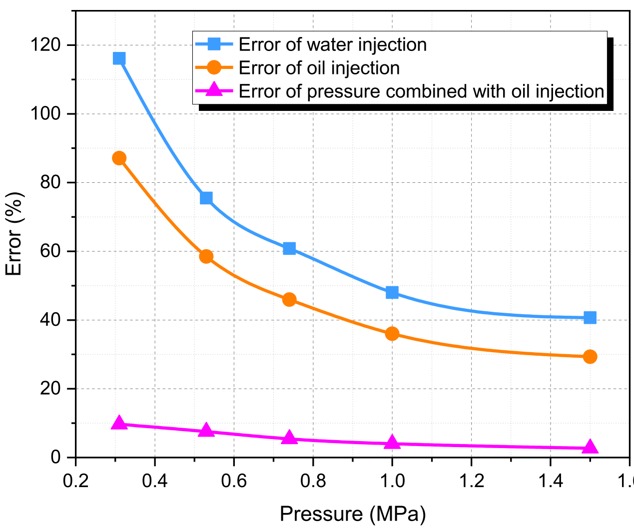

Figure 19. Pressure recovery error of three recovery methods.

https://doi.org/10.1021/acsomega.2c05120
ACS Omega 2022, 7, 41341−41352

recovered by stress loading alone, and the gas pressure recovery value after *in situ* volume recovery of the contact water injection and contact oil injection coal core is much larger than the initial adsorption equilibrium pressure. Obviously, using any of these three methods to recover the *in situ* volume of the coal core is not optimal.[58] However, the influence of a very small amount of silicone oil on gas adsorption of coal samples has been greatly reduced compared with complete oil injection and water injection, and the test error has been ideal, all within 10.00%. Therefore, the combination of contact oil injection and stress loading is feasible and the best way to recover the *in situ* volume of the coal core.

5. CONCLUSIONS

In this paper, a novel non-seal gas pressure measurement technology is proposed. Among them, the determination of the *in situ* volume restoration recovery is a key factor that affects the accuracy of the measurement results of this technology. This paper has carried out relevant experiments and studies on this key factor. The main findings of this study are as follows:

(1) This paper presents a new type of pressure measurement technology: the non-seal gas pressure measurement technology. This technology is mainly aimed at the three changes in coal samples before and after sampling and recovers the gas pressure at the pressure measurement location by compensating the gas leakage, restoring the *in situ* volume of the coal core, and simulating the reservoir temperature.

(2) In order to explore the best method to restore the *in situ* volume, we studied the restoration effects of four different *in situ* volume restoration methods: stress loading, contact water injection, contact oil injection, and the combination of stress loading and contact oil injection. It is found that the pressure error after restoring the *in situ* volume of the coal core by the combination of stress loading and contact oil injection is only between 2.67 and 9.68%, which is the best method to restore the original volume of the coal core. Besides, the stress loading method cannot completely recover the *in situ* volume of the coal core, but the recovery rate is 90%; the pressure error of using contact water injection to restore the *in situ* volume of the coal core is as high as 40.76 to 116.13%; the pressure recovery error in the contact oil injection is between 29.33 and 87.10%.

(3) The restoration of *in situ* volume increase in the coal core is realized, and the reliability of non-seal gas pressure measurement technology is improved. It provides a fast and reliable new way for the determination of the original gas pressure in coal mines, especially the residual gas pressure in coal seams after taking gas control measures.

■ AUTHOR INFORMATION

Corresponding Authors

Zhaofeng Wang − *State Collaboration Innovation Center of Coal Work Safety and Clean-efficiency Utilization, Jiaozuo 454000, China; College of Safety Science and Engineering, Henan Polytechnic University, Jiaozuo 454000, China; MOE Engineering Center of Mine Disaster Prevention and Rescue, Jiaozuo 454000, China;* orcid.org/0000-0003-1467-4893; Email: zhaofengw@hpu.edu.cn

Erlei Su − *State Collaboration Innovation Center of Coal Work Safety and Clean-efficiency Utilization, Jiaozuo 454000, China; State Key Laboratory Cultivation Base for Gas Geology and Gas Control, Henan Polytechnic University, Jiaozuo 454000, China; College of Safety Science and Engineering, Henan Polytechnic University, Jiaozuo 454000, China; MOE Engineering Center of Mine Disaster Prevention and Rescue, Jiaozuo 454000, China;* orcid.org/0000-0002-3165-6382; Email: suerlei1992@163.com

Authors

Chunlei Hua − *State Collaboration Innovation Center of Coal Work Safety and Clean-efficiency Utilization, Jiaozuo 454000, China; College of Safety Science and Engineering, Henan Polytechnic University, Jiaozuo 454000, China*

Jiaxin Dong − *College of Safety Science and Engineering, Henan Polytechnic University, Jiaozuo 454000, China*

Jiwei Yue − *College of Safety Science and Engineering, Henan Polytechnic University, Jiaozuo 454000, China*

Yongjie Cui − *Buertai Coal Mine, Shendong Coal Group, Inner Mongolia Ordos 017209, China*

Kangjia Zhang − *College of Safety Science and Engineering, Henan Polytechnic University, Jiaozuo 454000, China*

Complete contact information is available at: https://pubs.acs.org/10.1021/acsomega.2c05120

Notes

The authors declare no competing financial interest.

■ ACKNOWLEDGMENTS

This work is financially supported by the National Natural Science Foundation of China (52074107) and the State Key Laboratory Cultivation Base for Gas Geology and Gas Control (Henan Polytechnic University) (WS2021B11), which are gratefully acknowledged. Comments by all anonymous reviewers are highly appreciated.

■ REFERENCES

(1) Zhang, H.; Cheng, Y. P.; Deng, C. B.; Shu, L. Y.; Pan, Z. J.; Yuan, L.; Wang, L.; Liu, Q. Q. A Novel In-Seam Borehole Discontinuous Hydraulic Flushing Technology in the Driving Face of Soft Coal Seams: Enhanced Gas Extraction Mechanism and Field Application. *Rock Mech. Rock Eng.* **2022**, *55*, 885−907.

(2) Chu, Y. P.; Zhang, D. M.; Liu, H.; Wu, X. Y.; Zhai, P. P.; Sheng, T. Experimental study on mechanical properties, acoustic emission characteristics and energy evolution of coal samples after freezing with liquid nitrogen. *Fuel* **2022**, *321*, 123955.

(3) Xu, J. Z.; Zhai, C.; Ranjith, P. G.; Sang, S. X.; Sun, Y.; Cong, Y. Z.; Tang, W.; Zheng, Y. F. Investigation of the mechanical damage of low rank coals under the impacts of cyclical liquid CO2 for coalbed methane recovery. *Energy* **2022**, *239*, 122145.

(4) Su, E. L.; Liang, Y. P.; Chang, X. Y.; Zou, Q. L.; Xu, M. H.; Sasmito, A. P. Effects of cyclic saturation of supercritical CO_2 on the pore structures and mechanical properties of bituminous coal: An experimental study. *J. CO2 Util.* **2020**, *40*, 101208.

(5) Zou, Q.; Liu, H.; Zhang, Y. J.; Li, Q. M.; Fu, J. W.; Hu, Q. T. Rationality evaluation of production deployment of outburst-prone coal mines: A case study of nantong coal mine in Chongqing, China. *Saf. Sci.* **2020**, *122*, 104515.

(6) Lei, Y.; Cheng, Y. P.; Ren, T.; Tu, Q. Y.; Shu, L. Y.; Li, Y. X. The Energy Principle of Coal and Gas Outbursts: Experimentally Evaluating the Role of Gas Desorption. *Rock Mech. Rock Eng.* **2020**, *54*, 11−30.

(7) Lu, S. Q.; Wang, C. F.; Liu, Q. Q.; Zhang, Y. L.; Liu, J.; Sa, Z. Y.; Wang, L. Numerical assessment of the energy instability of gas outburst of deformed and normal coal combinations during mining. *Process Saf. Environ. Prot.* **2019**, *132*, 351−366.

(8) Zhao, W.; Cheng, Y. P.; Jiang, H. N.; Jin, K.; Wang, H. F.; Wang, L. Role of the rapid gas desorption of coal powders in the development stage of outbursts. *J. Nat. Gas Sci. Eng.* **2016**, *28*, 491−501.

(9) Wang, L.; Lu, Z.; Chen, D. P.; Liu, Q. Q.; Chu, P.; Shu, L. Y.; Ullah, B.; Wen, Z. J. Safe strategy for coal and gas outburst prevention in deep-and-thick coal seams using a soft rock protective layer mining. *Saf. Sci.* **2020**, *129*, 104800.

(10) Black, D. Review of coal and gas outburst in Australian underground coal mines. *Int. J. Min. Sci. Technol.* **2019**, *29*, 815−824.

(11) Beamish, B. B.; Crosdale, P. J. Instantaneous outbursts in underground coal mines: An overview and association with coal type. *Int. J. Coal Geol.* **1998**, *35*, 27−55.

(12) Lin, J.; Ren, T.; Wang, G. D.; Booth, P.; Nemcik, J. Experimental investigation of N2 injection to enhance gas drainage in CO2-rich low permeable seam. *Fuel* **2018**, *215*, 665−674.

(13) An, F. H.; Cheng, Y. P. An explanation of large-scale coal and gas outbursts in underground coal mines: the effect of low-permeability zones on abnormally abundant gas. *Nat. Hazard. Earth Sys.* **2014**, *14*, 2125−2132.

(14) Liu, T.; Lin, B. Q.; Fu, X. H.; Liu, A. Mechanical criterion for coal and gas outburst: a perspective from multiphysics coupling. *J. Curr. Sci. Technol* **2021**, *13*, 1423.

(15) Su, E.; Liang, Y.; Zou, Q.; Niu, F.; Li, L. Analysis of effects of CO_2 injection on coalbed permeability: Implications for coal seam CO_2 sequestration. *Energy Fuel* **2019**, *33*, 6606−6615.

(16) Tong, X. W.; Brandt, M.; Yue, Y. M.; Ciais, P.; Jepsen, M. R.; Penuelas, J.; Wigneron, J. P.; Xiao, X. M.; Song, X. P.; Horion, S.; Rasmussen, K.; Saatchi, S.; Fan, L.; Wang, K. L.; Zhang, B.; Chen, Z. C.; Wang, Y. H.; Li, X. J.; Fensholt, R. Forest management in southern China generates short term extensive carbon sequestration. *Nat. Commun.* **2020**, *11*, 129.

(17) Miller, S. M.; Michalak, A. M.; Detmers, R. G.; Hasekamp, O. P.; Bruhwiler, L. M. P.; Schwietzke, S. China's coal mine methane regulations have not curbed growing emissions. *Nat. Commun.* **2019**, *10*, 303.

(18) Su, E. L.; Liang, Y. P.; Zou, Q. L.; Xu, M. H.; Sasmito, A. P. Numerical analysis of permeability rebound and recovery during coalbed methane extraction: Implications for CO_2 injection methods. *Process Saf. Environ. Prot.* **2021**, *149*, 93−104.

(19) Xu, J. H.; Kang, Y.; Wang, X. C.; Feng, G.; Wang, Z. F. Dynamic characteristics and safety criterion of deep rock mine opening under blast loading. *Int. J. Rock Mech. Min.* **2019**, *119*, 156−167.

(20) Wang, D. K.; Lv, R. H.; Wei, J. P.; Fu, Q. C.; Wang, Y. T.; Zhang, P.; Yu, C.; Yao, B. H. An experimental study of seepage properties of gas-saturated coal under different loading conditions. *Energy Sci. Eng.* **2019**, *7*, 799−808.

(21) Su, E. L.; Liang, Y. P.; Zou, Q. L. Structures and fractal characteristics of pores in long-flame coal after cyclical supercritical CO_2 treatment. *Fuel* **2021**, *286*, 119305.

(22) Yan, G. Q.; Gang, G.; Lin, L.; Du, W. Z.; Huang, Q. M. Direct fitting measurement of gas content in coalbed and selection of reasonable sampling time. *Int. J. Min. Sci. Technol.* **2017**, *27*, 299−305.

(23) Wang, C.; Li, X.; Xu, C. G.; Chen, Y. J.; Tang, Z. X.; Zhang, C.; Du, Y.; Gao, X. Y.; Jiang, C. L. Dynamic Characterization during Gas Initial Desorption of Coal Particles and Its Influence on the Initiation of Coal and Gas Outbursts. *Processes* **2021**, *9*, 1101.

(24) Wang, C. J.; Li, X. W.; Xu, C. H.; Niu, Y.; Chen, Y. J.; Yang, S. Q.; Zhou, B. Z.; Jiang, C. L. Study on factors influencing and the critical value of the drilling cuttings weight: an index for outburst risk prediction. *Process Saf. Environ. Prot.* **2020**, *140*, 356−366.

(25) Diamond, W. P.; Schatzel, S. J. Measuring the gas content of coal: A review. *Int. J. Coal Geol.* **1998**, *35*, 311−331.

(26) Liu, P.; Fan, J. Y.; Jiang, D. Y.; Li, J. J. Evaluation of underground coal gas drainage performance: mine site measurements and parametric sensitivity analysis. *Process Saf. Environ. Prot.* **2021**, *148*, 711−723.

(27) Cui, X.; Zhang, J. Y.; Guo, L. W.; Gong, X. M. A New Method for the Measurement of Gas Pressure in Water-Bearing Coal Seams and Its Application. *Geofluids* **2020**, *2020*, 8881063.

(28) Wang, L.; Wang, Z. F.; Liu, H.; Chen, J. S.; Yang, T. L. An improvement sealing method for gas pressure measurement by drilling a reducing-nipple borehole. *Energy Sci. Eng.* **2018**, *6*, 595−606.

(29) Si, L.; Xi, Y.; Wei, J.; Li, B.; Wang, H. Y.; Yao, B. H.; Liu, Y. Dissolution characteristics of gas in mine water and its application on gas pressure measurement of water-intrusion coal seam. *Fuel* **2022**, *313*, 123004.

(30) Wang, L.; Cheng, L. B.; Cheng, Y. P.; Liu, S. M.; Guo, P. K.; Jin, K.; Jiang, H. N. A new method for accurate and rapid measurement of underground coal seam gas content. *J. Nat. Gas Sci. Eng.* **2015**, *26*, 1388−1398.

(31) Skiba, M.; Dutka, B.; Młynarczuk, M. MLP-Based Model for Estimation of Methane Seam Pressure. *Energies* **2021**, *14*, 7661.

(32) Wang, H.; Wang, E. Y.; Li, Z. H.; Shen, R. X.; Liu, X. F. Study and application of a new gas pressure inversion model in coal seam while drilling based on directional drilling technology. *Fuel* **2021**, *306*, 121679.

(33) Smith, D.; Williams, F. Diffusion models for gas production from coalsApplication to methane content determination. *Fuel* **1984**, *63*, 251−255.

(34) Smith, D. M.; Williams, F. L.A New Technique for Determining the Methane Content of Coal. *Proceedings Intersociety Energy Conversion Engineering Conference; (United States)*, 1981.

(35) Wang, L.; Cheng, Y. P.; Wang, L.; Guo, P. K.; Li, W. Safety line method for the prediction of deep coal-seam gas pressure and its application in coal mines. *Saf. Sci.* **2012**, *50*, 523−529.

(36) Zhao, W.; Wang, K.; Ju, Y.; Dong, H. Z.; Lou, Z.; An, F. H.; Feng, B. Influence of the roadway exposure time on the accuracy of gas content measurements in reconstructed and extended mines. *Process Saf. Environ. Prot.* **2020**, *142*, 109−117.

(37) Liu, Q. Q.; Cheng, Y. P. Measurement of pressure drop in drainage boreholes and its effects on the performance of coal seam gas extraction: a case study in the Jiulishan Mine with strong coal and gas outburst dangers. *Nat. Hazards* **2014**, *71*, 1475−1493.

(38) Cui, Y. J.; Wang, Z. F.; Fan, D. P. Feasibility study on gas pressure measurement technology of coal seam without sealing hole. *Coal Mines Saf.* **2021**, *11*, 22−27.

(39) Wang, L.; Wang, Z. F.; Qi, C. J.; Ma, S. J.; Yue, J. W. Physical Simulation of Temperature and Pressure Evolvement in Coal by Different Refrigeration Modes for Freezing Coring. *ACS Omega* **2019**, *4*, 20178−20187.

(40) Wang, Z. F.; Liang, J. N.; Yu, R.; Wang, Q. Study on the Equivalent Average Temperature Variation of the Coal Core during the Freeze Coring Process. *ACS Omega* **2022**, *7*, 3557−3567.

(41) Wang, Q.; Wang, Z. F.; Ma, S. J.; Zhang, K. J. Study on temperature variation of coal sample in process of freezing coring. *China Saf. Sci. J.* **2021**, *02*, 76−81.

(42) Wang, Z. F.; Wang, L.; Dong, J. X.; Wang, Q. Simulation on the temperature evolution law of coal containing gas in the freezing coring process. *J. China Coal Soc.* **2021**, *01*, 199−210.

(43) Maffioli, C. S. "Acqua premuta". Benedetto Castelli and the incompressibility of water. *B. Stor. Sci. Mat.* **2008**, *28*, 9−50.

(44) Franta, M.; Málek, J.; Rajagopal, K. R. Oil steady flows of fluids with pressure-and shear-dependent viscosities. *Proc. R. Soc. A* **2005**, *461*, 651−670.

(45) Cai, Y. D.; Liu, D. M.; Yao, Y. B.; Li, J. Q.; Liu, J. L. Fractal Characteristics of Coal Pores Based on Classic Geometry and Thermodynamics Models. *Acta Geol. Sin.* **2011**, *85*, 1150−1162.

(46) Peng, R. D.; Ju, Y.; Gao, F.; Xie, H. P.; Wang, P. Energy analysis on damage of coal under cyclical triaxial loading and unloading conditions. *J. China Coal Soc.* **2014**, *39*, 245−252.

(47) Jia, T.-R.; Zhang, Z. M.; Tang, C. A.; Zhang, Y. J. Numerical simulation of stress-relief effects of protective layer extraction. *Arch. Min. Sci.* **2013**, *58*, 521−540.

(48) Sun, Y. F.; Zhao, Y. X.; Wang, X.; Peng, L.; Sun, Q. Synchrotron radiation facility-based quantitative evaluation of pore structure heterogeneity and anisotropy in coal. *Pet. Explor. Dev.* **2019**, *46*, 1195−1205.

(49) Wang, Z. F.; Su, W. W.; Tang, X.; Wu, J. H. Influence of water invasion on methane adsorption behavior in coal. *Int. J. Coal Geol.* **2018**, *197*, 74−83.
(50) Wang, L.; Wang, Z. F.; Liu, H.; Chen, J. S.; Yang, T. L. An improvement sealing method for gas pressure measurement by drilling a reducing-nipple borehole. *Energy Sci. Eng.* **2018**, *6*, 595−606.
(51) Wu, J. H.; Yu, J. C.; Wang, Z. F.; Fu, X. H.; Su, W. W. Experimental investigation on spontaneous imbibition of water in coal: Implications for methane desorption and diffusion. *Fuel* **2018**, *231*, 427−437.
(52) Tian, Y.; Yan, C. H.; Jin, Z. H. Characterization of Methane Excess and Absolute Adsorption in Various Clay Nanopores from Molecular Simulation. *Sci. Rep.* **2017**, *7*, 12040.
(53) Wu, K.; Chen, Z. X.; Li, X. F.; Dong, X. H. Methane storage in nanoporous material at supercritical temperature over a wide range of pressures. *Sci. Rep.* **2016**, *6*, 33461.
(54) Yue, J.; Wang, Z. F.; Shi, B. M.; Dong, J. X.; Shen, X. J. Interaction mechanism of water movement and gas desorption during spontaneous imbibition in gas-bearing coal. *Fuel* **2022**, *318*, 123669.
(55) Jin, Z. H. Effect of nano-confinement on high pressure methane flow characteristics. *J. Nat. Gas Sci. Eng.* **2017**, *45*, 575−583.
(56) Zhang, J. F.; Clennell, M. B.; Dewhurst, D. N.; Liu, K. Y. Combined Monte Carlo and molecular dynamics simulation of methane adsorption on dry and moist coal. *Fuel* **2014**, *122*, 186−197.
(57) Zhang, J. X.; Gai, M. Y.; Ignatov, A. V.; Dyakov, S. A.; Wang, J.; Gippius, N. A.; Frueh, J.; Sukhorukov, G. B. Stimuli-Responsive Microarray Films for Real-Time Sensing of Surrounding Media, Temperature, and Solution Properties via Diffraction Patterns. *ACS Appl. Mater. Interfaces* **2020**, *12*, 19080−19091.
(58) Früh, A.; Rutkowski, S.; Akimchenko, I. O.; Tverdokhlebov, S. I.; Frueh, J. Orientation Analysis of Polymer Thin Films on Metal Surfaces via IR Absorbance of the Relative Transition Dipole Moments. *Appl. Surf. Sci.* **2022**, *594*, 153476.

https://doi.org/10.1021/acsomega.2c05120
ACS Omega 2022, 7, 41341−41352